Spatial correlation of temperature in turbulent Rayleigh-Bénard convection

T. Haramina and A. Tilgner
Institute of Geophysics, University of Göttingen, Friedrich-Hund-Platz 1, 37077 Göttingen, Germany
(Received 24 November 2005; revised manuscript received 13 September 2006; published 5 December 2006)

A cubic Rayleigh-Bénard cell is operated at a Rayleigh number of 1.5×10^9 and a Prandtl number of 6.1. The cell is equipped with thermistors placed along the vertical line through the center of the cell. The spatial correlation of temperature is deduced from simultaneous temperature recordings from these thermistors. The correlation function is well fitted by the sum of two exponentials. There is no cascade in the temperature field as only two characteristic length scales appear. The direct measurement of spatial correlations allows us to test the validity of Taylor's hypothesis in this flow.

DOI: 10.1103/PhysRevE.74.066304 PACS number(s): 47.27.T−, 44.25.+f

I. INTRODUCTION

Rayleigh-Bénard convection is one of the best studied model systems of turbulence. The turbulent fluctuations of velocity and temperature are usually characterized by their spectra. The classical theoretical work focuses on homogeneous turbulence and makes predictions on the spectral distribution of kinetic energy and temperature fluctuations as a function of (spatial) wave number. Two problems arise when comparing theory with experiment. First, real flows are never homogeneous. In the case of Rayleigh-Bénard convection in cubes or cylinders of modest aspect ratio (which are the most frequently used geometries), a large scale circulation develops. In a cubic cell, the flow is organized in a single roll oriented along the diagonal of the cell. The mean velocity is zero in the center of the cell and maximum in the vicinity of the walls. Second, most experiments record velocity or temperature at a fixed point in space and yield spectra as a function of frequency, not wave number. The translation from temporal to spatial domain requires the Taylor hypothesis which assumes that an advection velocity sweeps turbulent fluctuations past a stationary probe fast enough so that the fluctuations can be regarded as frozen in the fluid. Temperature measurements in highly turbulent Rayleigh-Bénard convection have revealed spectra which agree with the theoretically predicted Bolgiano spectrum if the Taylor hypothesis is assumed to be valid [1–3]. However, these spectra have also been observed in the center of the large scale roll where the average advection velocity is zero. It is thus of interest to directly measure the spatial spectrum of temperature fluctuations, or alternatively, the spatial correlation function, along the central axis of the cell. Direct measurements of spatial temperature spectra were performed before using optical scanning [4,5] which results in the spectrum spatially averaged along the laser beam. The method has the advantage that the spatial resolution is very high and the disadvantage that the temperature field is not truly local as the one obtained using thermistors.

The measurements reported in this paper investigate a single state with Rayleigh number 1.5×10^9 and Prandtl number 6.1. The temperature fluctuations are measured along the central axis of the cell along which the mean advection velocity is zero and the flow is neither homogeneous nor isotropic. The temporal spectra in this state do not show the Bolgiano spectrum with its characteristic power-law dependence indicative of a fully developed cascade, but the spectrum is broad and covers all frequencies from zero up to the dissipative range. Other features, such as the histogram of temperature fluctuations and the scaling of the heat transport with Rayleigh number are already the same as in more turbulent states [6–8]. The Reynolds number of the flow under consideration is 1200 based on the maximum velocity and the height of the cell.

Thermal boundary layers form at the top and bottom boundaries of a convection cell. Coherent structures are associated with those boundary layers, most importantly plumes. These objects have the shape of mushrooms in visualizations using shadowgraph or thermochromic liquid crystals [9,10]. Most of them are swept by the large scale flow towards the sidewalls while they move vertically away from the thermal boundary layers, so that only few traverse the center of the cell. Histograms of temperature fluctuations near the boundaries carry the signature of plumes and are skewed. The skewness decreases towards the center of the cell where the histograms are symmetric and exponential [11–13]. This, together with the broadband spectrum, suggests that structures of all scales should exist in the center of the cell. The correlation measurements reported here show that on the contrary, structures of only two different sizes dominate the temperature field. This is compatible with the claim that in turbulent flows the large and small scales are strongly coupled and that the traditional cascade picture is a crude representation of such flows as expressed in the review paper [14].

II. EXPERIMENTAL APPARATUS

The convection cell is the same as used in [15]. A cubic cell of height $d=20$ cm with Plexiglas sidewalls and silver coated copper plates at the top and bottom is electrically heated from below and water cooled from above. The cell is filled with water. The temperature of the bottom and top plates are typically set to 30 °C and 20 °C, respectively, so that the temperature difference Δ is $\Delta=10$ °C. Let ν, κ, and α be the viscosity, thermal diffusivity, and thermal expansion coefficient of water, and denote by G the gravitational acceleration. Using the material properties at the center of the cell, the Rayleigh number $\mathrm{Ra}=G\alpha\Delta d^3/(\kappa\nu)$ and Prandtl number $\mathrm{Pr}=\nu/\kappa$ are $\mathrm{Ra}=1.5\times10^9$ and $\mathrm{Pr}=6.1$.

Temperature profiles were measured using thermistors with a diameter of 400 μm. Each thermistor was individually calibrated against a digital thermometer with a 100 Ω sensing element. A thermistor was connected to a Wheatston bridge as a resistance arm and the temperature was calculated from the resistivity of the thermistor using a previously determined calibration curve. Nine thermistors have been placed on a vertical rod through the center of the cell, each 2 cm apart. The lower- and uppermost thermistors were 2 cm away from the plates. Together with thermistors in the plates, it was possible to measure at every instant the temperature profile along the center line with a resolution of 2 cm. In addition, another movable thermistor was available that could be translated vertically along the center line using a translation table mounted on the top of the upper plate. This made it possible to calculate the correlation with a 1 mm resolution at the points of interest. Correlations were measured by recording time series of all thermistors simultaneously for 2 h before shifting the movable thermistor to the next position. The sampling frequency was 4.4 Hz which ensured that the power spectra cover the whole range of frequencies up to the dissipation range. Additionally it ensured that the 50 Hz disturbance from the electrical network (and some other disturbances) are aliased to the high-frequency end of the spectra, so that they do not influence the analysis. The correlation between the fixed thermistors is known with better accuracy than the correlation between a fixed thermistor and the movable thermistor because of the longer accumulation time.

III. SPATIAL CORRELATION

Denote by $T_i(t)$ and $T_j(t)$ the temperatures at thermistors i and j as a function of time t, and by z the distance from the bottom plate, so that z_i and z_j are the positions of the two thermistors. One obtains from the two time series the correlation

$$g(z_i,\Delta z) = \frac{\langle T_i T_j \rangle}{\sqrt{\langle T_i^2 \rangle \langle T_j^2 \rangle}}, \tag{1}$$

where the brackets stand for time averages. The second argument of the correlation function g is the vertical separation of the points between which the correlation is measured, $\Delta z = z_j - z_i$. Because the flow is not homogeneous, the correlation depends not only on Δz but also on z_i. It is obvious from the definition of g that $g(z_i,\Delta z) = g(z_j,-\Delta z)$, or in general, $g(z,\Delta z) = g(z+\Delta z,-\Delta z)$. It will turn out that we can make the assumption that $g(z,\Delta z) \approx g(z,-\Delta z)$ or $g(z,\Delta z) \approx g(z,|\Delta z|)$. This assumption is certainly satisfied for $z = d/2$. It is also justified for small Δz at any position z if the flow is nearly homogeneous over the length Δz. For large Δz, when inhomogeneity certainly plays a role, either $z+\Delta z$ or $z-\Delta z$ is likely to lie outside the fluid, so that the correlation can be computed only on one side, anyway. That is why it is enough to present the results in terms of $g(z,|\Delta z|)$. This function is shown for three different values of z in Fig. 1. The fact that there are no significant outliers in these graphs shows that it is reasonable to use $|\Delta z|$ as argument in g. It is

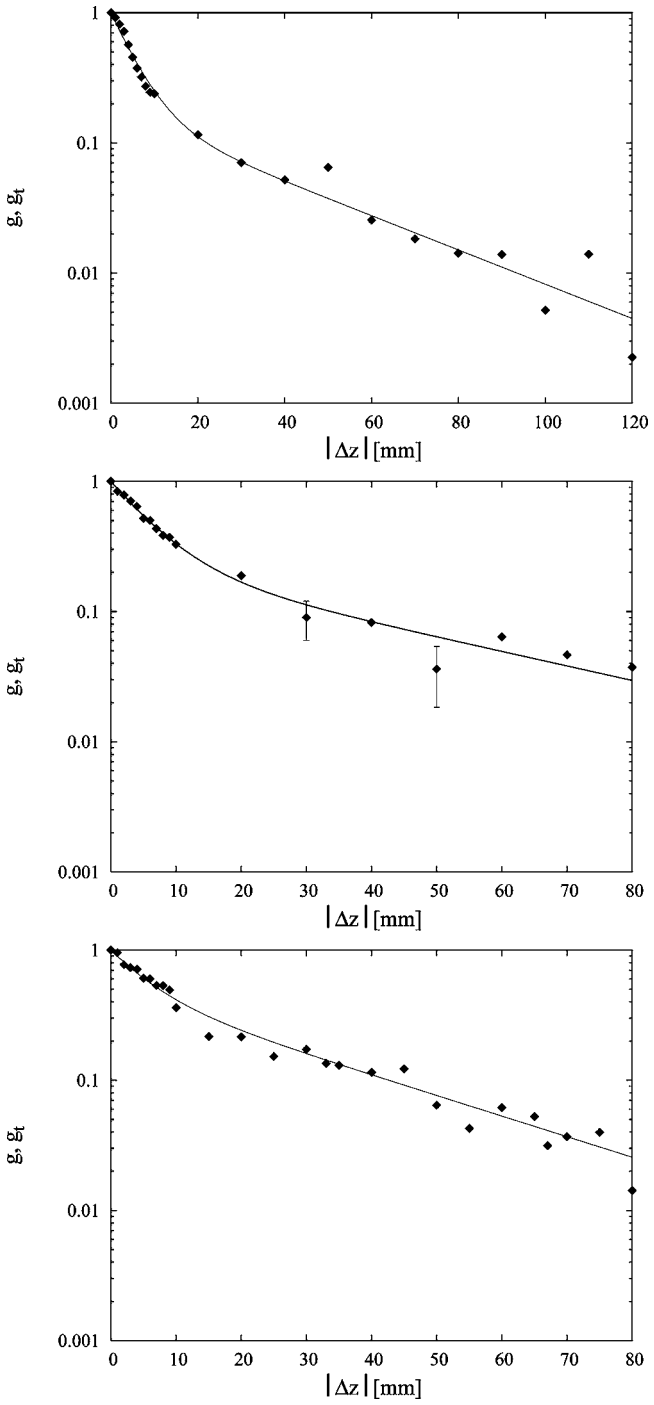

FIG. 1. The correlation function $g(z,|\Delta z|)$ (diamonds) for $z = 20$ mm, 60 mm, and 100 mm (from top to bottom) and the fitted g_t (solid line).

seen that at every position, the spatial correlation is the sum of two exponentials. The decay lengths of the two exponentials differ by an order of magnitude.

The measured correlation functions are well fitted by the function

$$g_t(z,|\Delta z|) = a_0(z) e^{-|\Delta z|/L_1(z)} + [1 - a_0(z)] e^{-|\Delta z|/L_2(z)}. \tag{2}$$

This functional form guarantees $g_t(z,0) = 1$. The two correlation lengths, L_1 and L_2, are shown as a function of z in Fig.

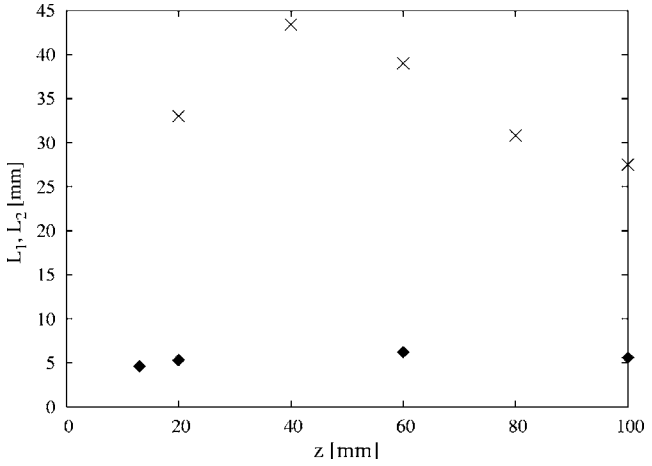

FIG. 2. The correlation lengths L_1 (diamonds) and L_2 (crosses) as a function of z.

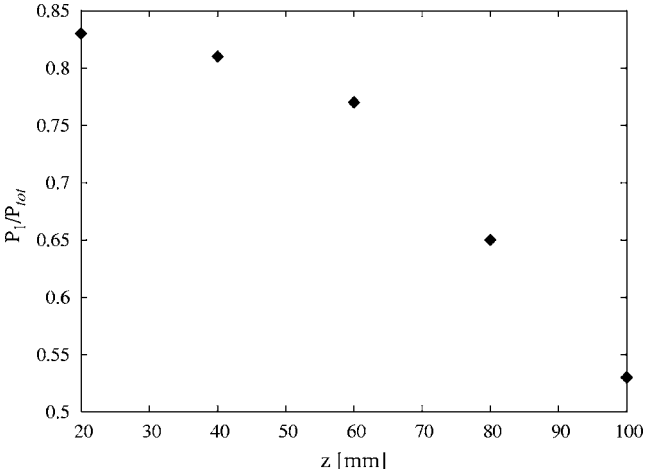

FIG. 3. The relative contribution of the small structures to the total power, P_1/P_{tot}, as a function of z.

2. The most immediate interpretation for the two terms in Eq. (2) is that they are related to two types of coherent structures of sizes L_1 and L_2. The smaller of the two lengths, L_1, is approximately independent of z with $L_1 \approx 5$ mm. The larger of the two lengths, L_2, reaches a maximum of 44 mm at $z=40$ mm and decreases approximately linearly with z at $z>40$ mm to reach a minimum of 28 mm in the center of the cell.

The small scale structures contribute an important fraction to the total rms of temperature even in the center of the cell. If we assume g_t to be an accurate representation of the true correlation function, we can compute the spatial spectrum $P(z,k)$ by

$$P(z,k) = 2\int_0^\infty g_t(z,|\Delta z|)e^{-ik|\Delta z|}d|\Delta z| = 2\left[\frac{a_0 L_1}{1+(kL_1)^2} + \frac{(1-a_0)L_2}{1+(kL_2)^2}\right]. \quad (3)$$

The rms of temperature at position z is given by $P_{tot} = \frac{1}{\pi}\int_0^\infty P(z,k)dk$, which naturally decomposes into the sum of two terms, P_1 and P_2, due to structures of size L_1 and L_2. The first term is

$$P_1 = \frac{1}{\pi}\int_0^\infty \frac{2a_0 L_1}{1+(kL_1)^2}dk = a_0, \quad (4)$$

and correspondingly, $P_2 = 1 - a_0$. The small scale structures thus contribute the fraction a_0 to the temperature fluctuations. Figure 3 shows P_1/P_{tot} as a function of z. Roughly half the fluctuations in the center are due to small scale structures.

There is no obvious reason why the correlation should decay exponentially rather than according to some other function. It is actually clear on theoretical grounds that g_t must be a poor fit in the neighborhood of $\Delta z=0$. The derivative of g_t with respect to Δz is not defined at $\Delta z=0$. On the other hand, the symmetry of the true correlation function, together with the smoothness of the temperature field, requires the derivative of the correlation function to vanish at $\Delta z=0$.

The rest of this section will discuss two structures occurring in convection cells in order to show that L_1 is not unreasonably small and to hint at possible origins of L_1. The structures of size L_1 are much more frequent near the plates than far away from the plates since the coefficient $a_0(z)$ varies from 0.83 at $z/d=0.1$ to 0.53 at the middle of the cell at $z/d=0.5$. The thickness of the thermal boundary layer in this cell is 2 mm. It could thus be that structures of size L_1 develop from boundary layer detachments which then drift into the bulk of the cell. At the same time, it is well known that passive scalars in turbulent velocity fields form narrow fronts. The gradient of the scalar is small inside advecting eddies and large on separatrices in between eddies. This mechanism leads to typical cliff-ramp structures in time series of the passive scalar [16]. The thickness of these fronts, or the dissipation length, is given by $d/\mathrm{Pe}^{1/2}$, where Pe is the Peclet number of the flow [16]. This length is 2.3 mm in the present flow. Time series of temperature recorded at isolated points cannot trace the history of the small scale structures (do they detach from the boundary layers or are they created in the bulk?). However, one can search for cliff-ramp structures in the time series. While some of them appear, they are much less frequent than symmetric excursions of temperature characteristic of plumes. The scaling of L_1 with Ra would test the hypothesis that L_1 is related to the thermal boundary layer thickness. The cell used here does not allow us to scan Ra over a significant interval.

IV. TEMPORAL SPECTRA

The most straightforward characterization of the time series $T_i(t)$ is to compute power spectra as a function of frequency f. Temporal and spatial spectra are simply related if there is an advection velocity v large enough so that Taylor's hypothesis holds. Wave number k and frequency f are then connected by $k=2\pi f/v$ and the temporal spectrum at position z, $\hat{P}(z,f)$, is given by

$$\hat{P}(z,f) = \frac{1}{v}P(z,2\pi f/v). \quad (5)$$

In Refs. [4,5] temporal and spatial (horizontal) power spectra were compared in a rectangular cell with aspect ratios $\Gamma_x=4$, $\Gamma_y=1$ at positions $d/50$ and $d/4$ (d being the height of the cell) from the plate. In these regions the mean advection velocity is well defined and it was shown that a sort of Taylor hypothesis is valid if v is taken to be the mean velocity. In the following we will test the hypothesis along the central vertical axis where the mean vertical velocity is zero. Figure 4 compares the measured temporal spectra together with those computed from Eqs. (2), (3), and (5). The values of a_0, L_1, and L_2 are those obtained from fitting g_t to the measured correlation function g. $\hat{P}$ is computed from g_t instead of g because there are not enough points in g for an accurate Fourier transform. At every position z, an advection velocity v is chosen in order to obtain the best possible fit of $\hat{P}$ to the measured temporal spectrum. As is seen in Fig. 4, the fit is good in the inertial range and discrepancies appear in the high frequency range. (On the integral scale the flow cannot be considered "frozen" so we ignore this range in the discussion.) The frequencies at which the spectra are poorly fitted correspond to certain separations Δz via the Taylor hypothesis. Even at those separations, g_t is a good fit to g, so that the discrepancies between $\hat{P}$ and the experimental spectra must be due to a failure of the Taylor hypothesis rather than to errors introduced by transforming the wrong correlation function. The condition for the Taylor hypothesis to hold is $T_{adv}/\tau \to 0$ where τ is the lifetime of the eddy advected by flow and T_{adv} is the time it takes the flow to advect the eddy past the probe. Assuming the simple Kolmogorov model, in the inertial range $T_{adv}/\tau \propto R^{1/3}$ where R is the size of the eddy. This implies that the smaller the eddy the closer we are to the conditions needed for the Taylor hypothesis to be valid. On the other hand, in the dissipation range the lifetime τ of an eddy is determined by the viscosity, $\tau \propto R^2/\nu$, which makes the ratio $T_{adv}/\tau \propto R^{-1}$. That is, in the dissipation range, the smaller the eddy the larger the ratio T_{adv}/τ which causes the Taylor hypothesis to fail in the high-frequency range.

Spatial measurements would be redundant if Taylor's hypothesis was strictly applicable, which it is not. It is thus necessary to measure the spatial correlation function in order to see that only two length scales characterize the flow. This information is blurred in the temporal spectra.

Finally, it is of interest to compare the $v(z)$ obtained from the fits with other velocities. The velocity in the large scale circulation is zero in the center of the cell, so that this velocity cannot be responsible for the approximate validity of the Taylor hypothesis at low frequencies, at least not in the center of the cell. Turbulent velocities themselves could also provide the necessary advection. In [18] it was found based on a theoretical model that the effective advection velocity one should use for the Taylor hypothesis is

$$v_{eff} = \sqrt{\bar{V}_0^2 + (bv_{rms})^2}, \tag{6}$$

where $\bar{V}_0$ is the mean large scale velocity, v_{rms} is the rms of velocity and b is a numerical factor, which was calculated to be between 3.1 and 4.2. In our case $\bar{V}_0=0$ so that Eq. (6) reduces to

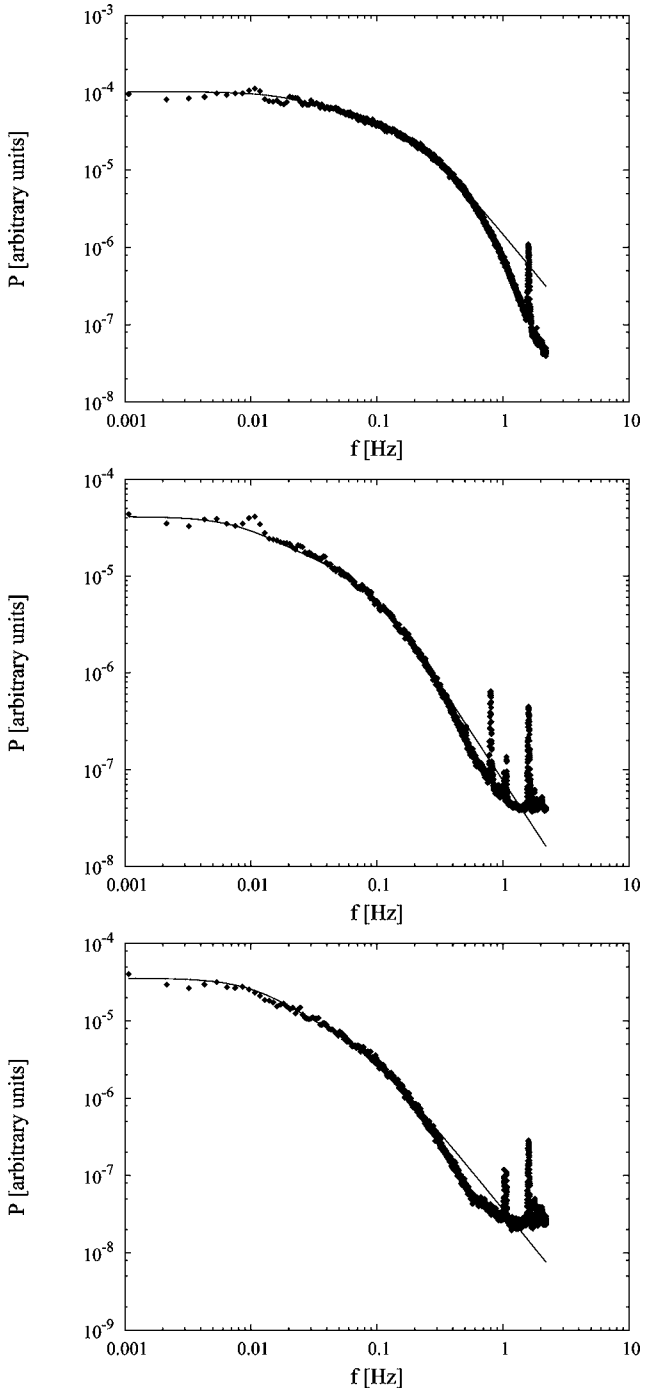

FIG. 4. Measured temporal spectra (diamonds) for $z=20$ mm, 60 mm, and 100 mm (from top to bottom) together with the fitted $\hat{P}(z,f)$ (solid line).

$$v_{eff} = bv_{rms}. \tag{7}$$

The rms of velocity is compared with $v(z)$ in Fig. 5. The rms velocity data are known from [17] at similar Ra and Pr as used here but for a slightly smaller cell, so that all quantities have to be made nondimensional for comparison in this figure. $v(z)$ and the velocity rms have identical height dependences, $v(z)$ being about four times larger than the velocity

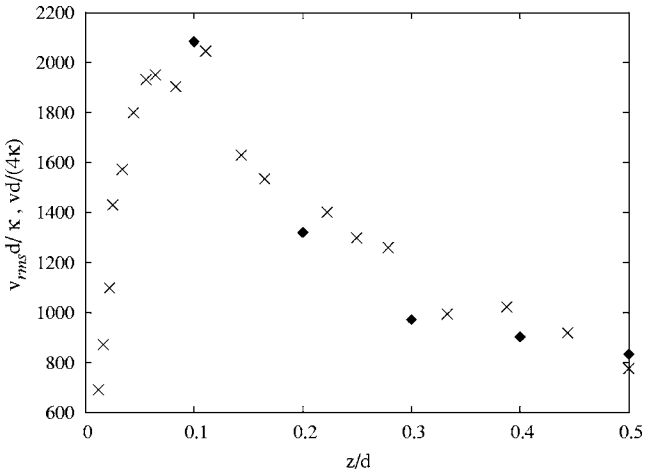

FIG. 5. The advection velocity v deduced from the fits of $\hat{P}(z,f)$ to the measured spectra (diamonds) together with the velocity rms, v_{rms} (crosses) as a function of the position in the cell.

rms. This is in excellent agreement with the theoretical prediction in [18].

V. CONCLUSION

In summary, it has been shown with measurements of spatial correlations of the temperature field that Rayleigh-Bénard convection at $\mathrm{Ra}=1.5\times10^9$ and $\mathrm{Pr}=6.1$ in a cubic cell has a bulk flow of surprisingly simple constitution. Two characteristic length scales occur in the correlation function of temperature which hints at the existence of two distinct coherent structures. There are structures of "large scale" which yield a temperature signal which decorrelates over a length in between 1/8 and 1/5 of the cell height, and structures of "small scale" with a correlation length about 2.5 times the thickness of the boundary layer, or equivalently, about 2.2 times the dissipation length of a passive scalar in the turbulent flow. The small scale structures are more frequent near the boundaries than in the bulk.

The Reynolds number of the flow, based on the size of the cell and the velocity of the large scale circulation, is 1200, which implies a Peclet number of 7300. It is striking that even at these parameters, the temperature field does not exhibit structures covering a broad range of sizes, but instead is dominated by only two length scales, and that there is not even a hint of a cascade. The temperature field directly carries the imprint of eddies with large Peclet number. However, it could be that the velocity field at small scales is more complex than the temperature field as heat diffusion can erase from the temperature field small scale structures present in the velocity field. In addition, thermal plumes emanating from the boundary layers possess large temperature gradients so that their temperature signal may hide weaker contributions created by advection in the bulk. Therefore, the fact that two length scales dominate the temperature field does not allow us to conclude that a broad range of scales is absent from the velocity field.

It is necessary to measure spatial correlation functions to reveal the simplicity of the flow. Temporal spectra, obtained from a single probe fixed in space, do not provide the same information because the Taylor hypothesis is not valid throughout the entire frequency range. In the inertial range, where the Taylor hypothesis is valid, the velocity used for transformation of spatial to temporal coordinates is about four times the velocity rms. Spectra recorded in more turbulent convective states than the one investigated here have shown power laws in the spectra of turbulent temperature fluctuations, suggesting a fully developed cascade. It will be an important task for the future to measure spatial correlation functions in these more turbulent states.

ACKNOWLEDGMENT

This work was supported by the "Deutsche Forschungsgemeinschaft."

[1] J. J. Niemela, L. Skrbek, K. R. Sreenivasan, and R. J. Donnelly, Nature (London) **404**, 837 (2000).
[2] X.-Z. Wu, L. Kadanoff, A. Libchaber, and M. Sano, Phys. Rev. Lett. **64**, 2140 (1990).
[3] F. Heslot, B. Castaing, and A. Libchaber, Phys. Rev. A **36**, 5870 (1987).
[4] F. Chillá, S. Ciliberto, C. Innocenti, and E. Pampaloni, Europhys. Lett. **22**, 23 (1993).
[5] F. Chillá, S. Ciliberto, C. Innocenti, and E. Pampaloni, Nuovo Cimento Soc. Ital. Fis., D **15**, 1229 (1993).
[6] R. J. Goldstein and S. Tokuda, Int. J. Heat Mass Transfer **23**, 738 (1980).
[7] S. L. Lui and K. Q. Xia, Phys. Rev. E **57**, 5494 (1998).
[8] X. L. Qiu and K. Q. Xia, Phys. Rev. E **58**, 486 (1998).
[9] G. Zocchi, E. Moses, and A. Libchaber, Physica A **166**, 387 (1990).
[10] H.-D. Xi, S. Lam, and K.-Q. Xia, J. Fluid Mech. **503**, 47 (2004).
[11] M. Sano, X. Z. Wu, and A. Libchaber, Phys. Rev. A **40**, 6421 (1989).
[12] B. Castaing, G. Gunaratne, F. Heslot, L. Kadanoff, A. Libchaber, S. Thomae, S. Zaleski, and G. Zanetti, J. Fluid Mech. **204**, 1 (1989).
[13] A. Belmonte, A. Tilgner, and A. Libchaber, Phys. Rev. E **50**, 269 (1994).
[14] Z. Warhaft, Annu. Rev. Fluid Mech. **32**, 203 (2000).
[15] T. Haramina and A. Tilgner, Phys. Rev. E **69**, 056306 (2004).
[16] B. Shraiman and E. D. Siggia, Nature (London) **405**, 639 (2000).
[17] A. Tilgner, A. Belmonte, and A. Libchaber, Phys. Rev. E **47**, R2253 (1993).
[18] V. S. L'vov, A. Pomyalov, and I. Procaccia, Phys. Rev. E **60**, 4175 (1999).